An Axisymmetric Inverse Approach for Cold Forging Modeling

Ali Halouani, Yuming Li, Boussad Abbès, Ying-Qiao Guo

Abstract— **This paper presents the formulation of an axi-symmetric element based on an efficient method called the "Inverse Approach" (I.A.) for the numerical modeling of cold forging process. In contrast to the classical incremental methods, the Inverse Approach exploits the known shape of the final part and executes the calculation from the final part to the initial billet. The assumptions of the proportional loading and the simplified tool actions make the I.A. calculation very fast. The metal's incompressibility is ensured by the penalty method. The comparison with Abaqus shows the efficiency and limitations of the I.A. which will be a good tool for the preliminary preform design.**

Index Terms— **Cold forging process, large strains, integrated constitutive law, axi-symmetrical element, Inverse Approach.**

I. INTRODUCTION

In a cold forging process, the metal is plastically deformed under the tool action. The forging process allows not only to change the billet's shape but also to improve the metal properties because it refines the metal grain size. Forged parts are often used for high performance and high reliability applications where the strength and the human safety are crucially important.

The numerical modelling plays an important role in the tool design for the forging process. Many research groups work on the forward method or on the backward tracing method for the forging simulation and optimization [4]-[7]. Very advanced works have been done by Chenot, Fourment et al. from CEMEF in France and the corresponding software "FORGE" is largely used in the forging industry.

Two simplified methods called Inverse Approach (I.A.) and Pseudo Inverse Approach (P.I.A.) have been developed by Batoz, Guo et al. [8], [9] for the sheet forming modeling. They are less accurate but much faster than classical incremental approaches.

Manuscript received March 18, 2010. This work was supported in part by French state and by Champagne-Ardenne Region under the Project OPOMEF their sponsor and financial support are gratefully acknowledged.

A. Halouani is with MAN/GRESPI, University of Reims Champagne-Ardenne, F51687 Reims, France (e-mail: ali.halouani@etudiant.univ-reims.fr).

Y. Li is with MAN/GRESPI, University of Reims Champagne-Ardenne, F51687 Reims, France (e-mail: yuming.li@univ-reims.fr).

B. Abbès is with MAN/GRESPI, University of Reims Champagne-Ardenne, F51687 Reims, France (corresponding author, phone: 33-3-26918135; fax: 33-3-26913803; email: boussad.abbes@univ-reims.fr).

Y.Q Guo is with MAN/GRESPI, University of Reims Champagne-Ardenne, F51687 Reims, France (email: yq.guo@univ-reims.fr).

The aim of the present work is to study the feasibility of the I.A. for the cold forging modeling. The formulation of an axi-symmetric element based on the I.A. is developed for the preliminary preform design and optimization.

In this study, firstly, we present the basic idea of the I.A. and the main steps of modelling. Then, we talk about the formulation of an axi-symmetric element based on the I.A.: the principle of virtual work in large deformation, the large logarithmic strains, the integrated constitutive law, the technique to ensure the incompressibility of the metal and the treatment of the boundary conditions. An example will be presented to show the efficiency and limitations of the present I.A. for the forging process modelling.

II. OUTLINE OF THE INVERSE APPROACH

The Inverse Approach is based on the knowledge of the final part shape. The prediction of the trajectories of all material points from the initial billet to the known final part is done in one step by comparing directly the initial and final configurations. Two basic assumptions are used in this study: the assumption of proportional loading (for cold forging) gives an integrated constitutive law without considering the strain path and the visco-plasticity, the assumption of contact between the part and tools allows one to replace the tool actions by nodal forces without contact treatment. These two assumptions make the I.A. calculation very fast.

The I.A. procedure is carried out as follows (Fig. 1):

1) The finite element mesh is created on the known final part.

2) As an initial solution, the nodes at the part contour are mapped on the contour of the initial billet and a linear resolution allows determining the positions of the other nodes (internal nodes) in the initial billet.

3) The large strains are calculated by using the Cauchy-Green left tensor between the two meshes, the stresses are obtained by using an integrated constitutive law.

4) An implicit Newton–Raphson algorithm is used to move the nodes in the initial billet in order to satisfy equilibrium in the final part.

ISBN: 978-988-18210-7-2
ISSN: 2078-0958 (Print); ISSN: 2078-0966 (Online)

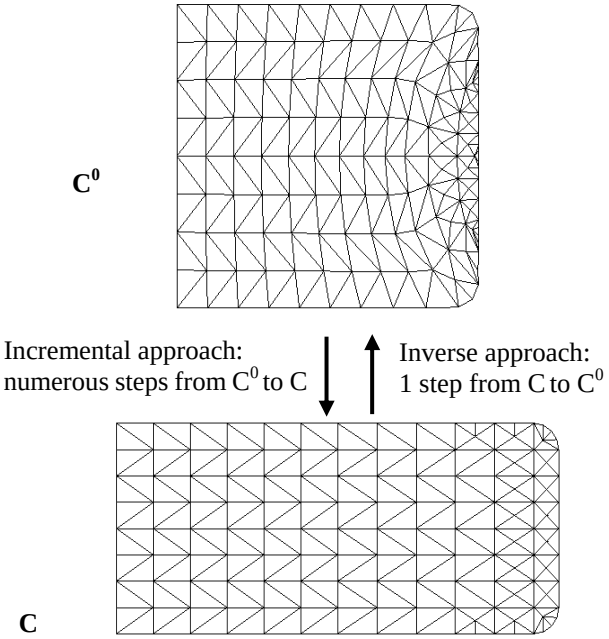

Fig. 1 Two approaches for forging process modelling

III. AXISYMMETRIC ELEMENT BASED ON I.A.

A. Principle of Virtual Work (PVW)

In the Inverse Approach, the final configuration is known and taken as reference configuration. The equilibrium of the final part is expressed by the principle of virtual work:

$$W = \sum_{\text{elt}} W^{\text{e}} = \sum_{\text{elt}} \left(W^{\text{e}}_{\text{int}} - W^{\text{e}}_{\text{ext}} \right) = 0 \tag{1}$$

with $W^{\text{e}}_{\text{int}} = \int_{v^e} \left\langle \varepsilon^* \right\rangle \{\sigma\}\, dv$ (2)

$$W^{\text{e}}_{\text{ext}} = \int_{v^e} \left\langle u^* \right\rangle \{f\}\, dv \tag{3}$$

$$\langle \sigma \rangle = \langle \sigma_x \quad \sigma_\theta \quad \sigma_z \quad \sigma_{xz} \rangle$$

$$\left\langle \varepsilon^* \right\rangle = \left\langle \varepsilon^*_x \quad \varepsilon^*_\theta \quad \varepsilon^*_z \quad \gamma^*_{rz} \right\rangle$$

where W^e_{int} and W^e_{ext} are the element internal and external virtual works, $\langle \sigma \rangle$ the Cauchy stresses, $\left\langle \varepsilon^* \right\rangle$ the virtual strains, $\left\langle u^* \right\rangle$ the virtual displacements, $\{f\}$ the volume forces.

We note that: the virtual strains are infinitesimal, so they are linear functions of virtual displacements; whereas, the above Cauchy stresses are related to the large strains, so generally they are calculated by an incremental algorithm. In the present study, a total method is proposed: 1) the deformation gradient tensor and the Cauchy-Green left tensor are defined; 2) then the principal elongations and large logarithmic strains are calculated; 3) finally the Cauchy stress is calculated by using an integrated constitutive law (Hencky-Mises).

B. Virtual strain operator

For an axi-symmetric problem, the strain vector is often defined in the global cylindrical coordinate system $(r, \theta, Z,$ Fig. 2). In our finite element formulation, it is more convenient to define the strains in the local element system (x, θ, z):

$$\left\{\varepsilon^*\right\} = \begin{Bmatrix} \varepsilon^*_x \\ \varepsilon^*_\theta \\ \varepsilon^*_z \\ \gamma^*_{xz} \end{Bmatrix} = \begin{Bmatrix} u^*_{,x} \\ \dfrac{u^* \cos\alpha - w^* \sin\alpha}{r} \\ w^*_{,z} \\ u^*_{,z} + w^*_{,x} \end{Bmatrix} \tag{4}$$

where u^* and w^* are the virtual displacements along x and z, r the radial coordinate and α is the inclination angle of the local reference with respect to the global reference ($(o, \vec{x})$ to $(o, \vec{r})$) .

The present element is an axi-symmetrical CST element with three nodes and six degrees of freedom. The displacements are interpolated linearly in terms of nodal displacements**:**

$$\begin{Bmatrix} u \\ w \end{Bmatrix} = \begin{bmatrix} N_1 & 0 & N_2 & 0 & N_3 & 0 \\ 0 & N_1 & 0 & N_2 & 0 & N_3 \end{bmatrix} \{u_n\} \tag{5}$$

$$\{u_n\} = \langle u_1 \quad w_1 \quad u_2 \quad w_2 \quad u_3 \quad w_3 \rangle^T$$

where $N_i(x,z)$ are the linear interpolation functions for an element.

Substituting Eq. (5) into (4), we obtain the following virtual strain operator $[B_m]$:

$$\left\{\varepsilon^*\right\} = [B_m] \left\{u^*_n\right\} \tag{6}$$

with

$$[B_m] = \begin{bmatrix} N_{1,x} & 0 & N_{2,x} & 0 & N_{3,x} & 0 \\ \dfrac{N_1 \cos\alpha}{r} & -\dfrac{N_1 \sin\alpha}{r} & \dfrac{N_2 \cos\alpha}{r} & -\dfrac{N_2 \sin\alpha}{r} & \dfrac{N_3 \cos\alpha}{r} & -\dfrac{N_3 \sin\alpha}{r} \\ 0 & N_{1,z} & 0 & N_{2,z} & 0 & N_{3,z} \\ N_{1,z} & N_{1,x} & N_{2,z} & N_{2,x} & N_{3,z} & N_{3,x} \end{bmatrix}$$

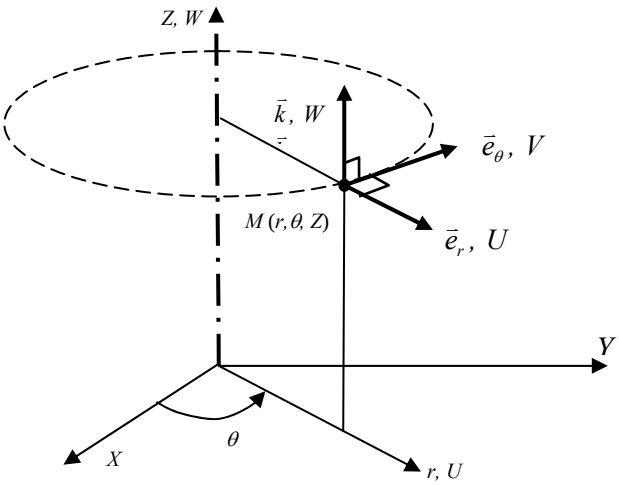

Fig. 2 Cylindrical coordinate system (r, θ, Z)

C. Internal force vector

Substituting Eq. (6) into (2) gives the element internal force vector in the local reference:

$$W_{\text{int}}^{\ e} = \left\langle u_n^* \right\rangle 2\pi \iint_{A^e} \left[B_m\right]^T \{\sigma\} r dA = \left\langle u_n^* \right\rangle \left\{F_{\text{int}}^{\ e}\right\} \quad (7)$$

Since the stress vector $\{\sigma\}$ is not constant in an element, generally we should introduce the reference element and use the numerical integration to calculate the internal force vector in the local reference. A reduced integration method is proposed by Batoz and Dhatt [2]: the stresses are supposed linear in an element and the barycentre is taken as single integration point. Thus the calculation of the internal force vector becomes very simple:

$$\left\{F_{\text{int}}^{\ e}\right\} = 2\pi A r_m \left[B_m\right]_{r_m}^T \{\sigma\} \quad (8)$$

with $r = r_{\text{m}} = \frac{1}{3}(r_1 + r_2 + r_3)$

D. External force vector

In a forging process, the initial billet is submitted to a normal pressure force and a tangential friction force on the contour. In the Inverse Approach, these tool actions are simply represented by some external nodal forces at the final configuration to avoid the contact treatment. At a node, the direction of the resultant force $\vec{n}_f$ can be defined by the friction cone and the slide direction:

$$\vec{n}_f = \frac{1}{\sqrt{1+\mu^2}}\left(\vec{n} - \mu\vec{t}\right) \quad (9)$$

where $\vec{n}$ is the unit normal vector of the contour, $\vec{t}$ the unit vector of the projection of the node displacement on the tangent direction of the contour, μ the friction coefficient.

The FE discretization allows one to establish the following equations representing the equilibrium on a node k:

$$\left\{F_{ext}^k(P^k)\right\} - \left\{F_{\text{int}}^i\right\} = \begin{Bmatrix} P^k n_r^k \\ P^k n_Z^k \end{Bmatrix}_{ext} - \begin{Bmatrix} F_r^k \\ F_Z^k \end{Bmatrix}_{int} = \begin{Bmatrix} 0 \\ 0 \end{Bmatrix} \quad (10)$$

where $\left\langle n_r^k \quad n_Z^k \right\rangle^T = \vec{n}_f$ represents the direction of the resultant force at the node *k* (Eq. 9), the intensity of this force P^k can be determined as follows:

$$P^k = \left\langle n_r^k \quad n_Z^k \right\rangle \begin{Bmatrix} F_r^k \\ F_Z^k \end{Bmatrix}_{int} \quad (11)$$

The element external force vector is finally obtained:

$$\left\{F_{ext}^k\right\} = \left\langle n_r^k \quad n_Z^k \right\rangle \begin{Bmatrix} F_r^k \\ F_Z^k \end{Bmatrix}_{int} \begin{Bmatrix} n_r^k \\ n_Z^k \end{Bmatrix} \quad (12)$$

E. Large logarithmic strains

In the Inverse Approach, we use an integrated constitutive law which associates the total strains to the total stresses. These large strains are calculated by the following steps: the inverse of deformation gradient tensor ➔ the inverse of the Cauchy-Green left tensor ➔ the principal elongations ➔ the logarithmic strains.

The word « inverse » is used to indicate that the known final configuration is taken as reference configuration, and the calculation is carried out from the known final part to the unknown initial billet.

The solid has an axis of revolution $(o, \vec{Z})$. Any point *M* in the solid is defined in the global reference by its cylindrical coordinates (*r, θ, Z,* Fig. 2). The displacement field is composed of the radial, circumferential and vertical displacements (*U, V, W*):

$$\vec{U} = U\vec{e_r} + V\vec{e_\theta} + W\vec{k} \quad (13)$$

This allows us to obtain the differential of the displacement field:

$$d\vec{U} = (dU - Vd\theta)\vec{e_r} + (dV + Ud\theta)\vec{e_\theta} + dW\vec{k} \quad (14)$$

For an axi-symmetric problem, each point of the solid moves in its meridian plane (*V=0*) and the displacement field is independent of the circumferential coordinate ($\frac{\partial}{\partial\theta} = 0$).

In this case, the displacement gradient tensor in cylindrical coordinates is reduced to:

$$\left[\frac{\partial \mathbf{U}}{\partial \mathbf{r}}\right] = \begin{bmatrix} U_{,r} & 0 & U_{,Z} \\ 0 & \frac{U}{r} & 0 \\ W_{,r} & 0 & W_{,Z} \end{bmatrix} \quad (15)$$

In our Inverse Approach in large strain and plasticity, it is more convenient to define the deformation gradient tensor in the element local system:

$$\left[F\right]_l^{-1} = \left(\left[I\right] - \left[\frac{\partial \mathbf{u}}{\partial \mathbf{x}}\right]\right) = \begin{bmatrix} 1-u_{,x} & 0 & -u_{,z} \\ 0 & 1-\frac{u\cos\alpha - w\sin\alpha}{r} & 0 \\ -w_{,x} & 0 & 1-w_{,z} \end{bmatrix} \quad (16)$$

where $\vec{u}$ is the displacement vector in the local reference from the initial position vector $\vec{x}^0$ to the final position vector $\vec{x}$.

F. Inverse of the Cauchy-Green left tensor

The inverse of the Cauchy-Green left tensor in the local system is determined by the following expression:

$$\left[B\right]^{-1} = \left[F\right]_l^{-T}\left[F\right]_l^{-1} = \begin{bmatrix} a & 0 & b \\ 0 & d & 0 \\ b & 0 & c \end{bmatrix} \quad (17)$$

The tensor $\left[B\right]^{-1}$ defined in the local reference can be transformed to the principal reference to obtain the three eigenvalue $(\lambda_1^{-2}, \lambda_2^{-2}, \lambda_3^{-2})$, then the three principal elongations $(\lambda_1, \lambda_2, \lambda_3)$:

$$\left[B\right]^{-1} = \left[M\right]\begin{bmatrix} \lambda_1^{-2} & 0 & 0 \\ 0 & \lambda_2^{-2} & 0 \\ 0 & 0 & \lambda_3^{-2} \end{bmatrix}\left[M\right]^T \quad (18)$$

with $\begin{Bmatrix} \lambda_1^{-2} \\ \lambda_3^{-2} \end{Bmatrix} = \left\{ \frac{a+c}{2} \pm \sqrt{\left(\frac{a-c}{2}\right)^2 + b^2} \right\}$ (19)

ISBN: 978-988-18210-7-2
ISSN: 2078-0958 (Print); ISSN: 2078-0966 (Online)

$$[M]=\begin{bmatrix}\cos\varphi & 0 & -\sin\varphi\\ 0 & 1 & 0\\ \sin\varphi & 0 & \cos\varphi\end{bmatrix} \quad (20)$$

where φ is the angle from the local reference to the principal reference.

Finally, the principal logarithmic strains are defined by:

$$\{\varepsilon\}=\begin{Bmatrix}\varepsilon_1\\ \varepsilon_2\\ \varepsilon_3\end{Bmatrix}=\begin{Bmatrix}Log\,\lambda_1\\ Log\,\lambda_2\\ Log\,\lambda_3\end{Bmatrix} \quad (21)$$

The assumption of incompressibility of the metal gives the volume strain null:

$$\varepsilon_v=\varepsilon_1+\varepsilon_2+\varepsilon_3=\varepsilon_x+\varepsilon_\theta+\varepsilon_z=0 \quad (22)$$

$$\lambda_1\lambda_2\lambda_3=\lambda_x\lambda_\theta\lambda_z=1 \quad (23)$$

G. Penalization method for metal incompressibility

The incompressibility of the metal can be ensured by introducing a Lagrange multiplier or a penalization term (Kobayashi and Altan, [5]). In our Inverse Approach, we add a penalization term in the Principle of Virtual Work:

$$W=\sum_{elt}\left(\int_{v^e}\langle\varepsilon^*\rangle\{\sigma\}\,dv-\int_{v^e}\langle u^*\rangle\{f\}\,dv+\int_{v^e}K\varepsilon_v^*\varepsilon_v\,dv\right)=0 \quad (24)$$

where ε_v is the volume strain, K is a great positive factor which allows to annul ε_v in the convergence loop. Using the virtual strains operator (Eq. 6), we obtain a vector of "equivalent forces" relative to the volume stain:

$$\varepsilon_v^*=\langle u_n^*\rangle[B_m]^T_{6\times3}\begin{Bmatrix}1\\1\\1\end{Bmatrix}=\langle u_n^*\rangle\{B_v\} \quad (25)$$

so $$\int_{v^e}K\,\varepsilon_v^*\,\varepsilon_v\,dv=\langle u_n^*\rangle\{F_v^e\}$$

$$\{F_v^e\}=2\pi r_m A K\{B_v\}_{r_m}(\varepsilon_x+\varepsilon_\theta+\varepsilon_z) \quad (26)$$

H. Integrated constitutive law (Hencky-Mises)

In the present study, the isotropic constitutive law is adopted. The Von Mises criterion of plasticity is expressed by:

$$f=\bar\sigma-\sigma_Y=(\langle\sigma\rangle[P]\{\sigma\})^{\frac12}-\sigma_Y=0 \quad (27)$$

with $\bar\sigma=\frac{\sqrt2}{2}\left[(\sigma_x-\sigma_\theta)^2+(\sigma_\theta-\sigma_z)^2+(\sigma_z-\sigma_x)^2+6\sigma_{xz}{}^2\right]^{\frac12}$

where $\bar\sigma$ is the equivalent stress, σ_Y the yield stress.

The normality law allows one to establish the relation between the plastic strain rate and the Cauchy stress using the plastic multiplier $\dot\lambda$:

$$\{\dot\varepsilon^p\}=\dot\lambda\frac{\partial f}{\partial\{\sigma\}}=\frac{\dot\lambda}{\bar\sigma}[P]\{\sigma\} \quad (28)$$

So $$\dot{\bar\varepsilon}^p=(\langle\dot\varepsilon^p\rangle[P]^{-1}\{\dot\varepsilon^p\})^{\frac12}=\dot\lambda \quad (29)$$

Using Eqs. (28) and (29), we obtain:

$$\{\dot\varepsilon^p\}=\frac{\dot{\bar\varepsilon}^p}{\bar\sigma}[P]\{\sigma\} \quad (30)$$

The Hencky assumption (proportional loading) allows to directly integrating the plastic strain rate:

$$\{\varepsilon^p\}=\int_0^t\{\dot\varepsilon^p\}dt=\frac{\bar\varepsilon^p}{\bar\sigma}[P]\{\sigma\}$$

$$=\frac{1}{H_s}[P]\{\sigma\}=(\frac{1}{E_s}-\frac{1}{E})[P]\{\sigma\} \quad (31)$$

where $E_s=\frac{\bar\sigma}{\bar\varepsilon}$ is the secant modulus of the uniaxial stress–strain curve.

Adding the elastic strains, we obtain the total strain:

$$\{\varepsilon\}=\{\varepsilon^p\}+\{\varepsilon^e\}=([C]+(\frac{1}{E_s}-\frac{1}{E})[P])\{\sigma\} \quad (32)$$

where $[C]$ is the elastic flexibility matrix.

Finally, the total Cauchy stresses are obtained in terms of the total logarithmic strains as:

$$\{\sigma\}=[H_{ep}]\{\varepsilon\}=([C]+(\frac{1}{E_s}-\frac{1}{E})[P])^{-1}\{\varepsilon\} \quad (33)$$

I. Boundary conditions on an irregular contour

In the present Inverse Approach, the displacements of the nodes at the contour are supposed tangential to the contour defined by the tools. Dhatt and Touzot [1] proposed to establish a contour reference and impose the normal displacements null in this reference.

Considering a node i on the contour of a mesh. We establish a contour reference defined by the tangential and normal directions in which we impose the normal displacement $V_i'=0$ (tangent displacement $U_i'\neq0$). The following matrix allows one to transform les displacements between the contour reference and global reference:

$$\begin{Bmatrix}U_i\\ V_i\end{Bmatrix}=\begin{bmatrix}\cos\alpha_i & -\sin\alpha_i\\ \sin\alpha_i & \cos\alpha_i\end{bmatrix}\begin{Bmatrix}U'_i\\ V'_i\end{Bmatrix} \quad (34)$$

It is more convenient to transform the tangent stiffness matrix and the vector of residual forces at the elementary level.

After the resolution, the displacements in the contour references should be re-transformed into the global reference.

IV. NUMERICAL RESULTS

The validation of the simplified Inverse Approach is done by using the code ABAQUS®/Explicit. Two axi-symmetric parts are considered.

ISBN: 978-988-18210-7-2
ISSN: 2078-0958 (Print); ISSN: 2078-0966 (Online)

A. *Numerical results of the part 1*

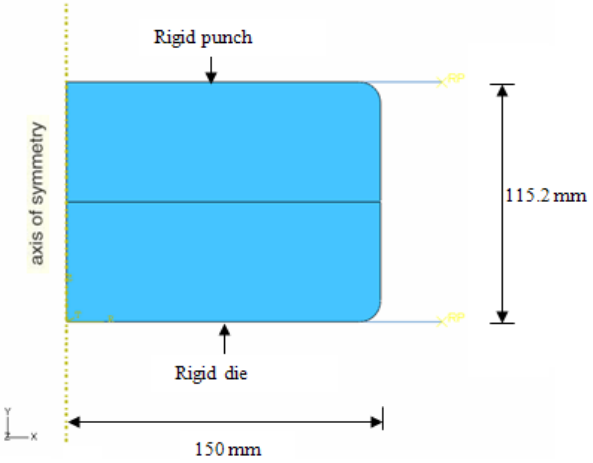

Fig. 3 Geometry of the part 1

The geometry of the part 1 is shown in Fig. 3. In the simulation by the incremental approach, the initial billet is discretized into 176 axi-symmetric triangle elements (CAX3 of Abaqus). The tools (punch and die) are supposed rigid and modeled by analytic rigid wire. One point of the tool surface was defined as reference point. The tools displacement was specified by using this point.

A master-slave contact approach is used in this simulation where the tools are considered as the master surfaces and the outer surface of the billet (surface facing the tools) constitutes the slave surface.

The material of the billet is the lead whose properties are: Young's modulus E=17 (GPa), Poisson's ratio ν=0.42, friction coefficient μ=0.35, Hollomon stress-strain curve $\bar{\sigma}=65.8\left(\bar{\varepsilon}^{p}\right)^{0.27}$ (MPa). The punch is moved vertically. The total punch travel is 3.52 (mm). In order to compare the two approaches, we mesh the billet (Fig. 4a) and use Abaqus to obtain the mesh of the final part (Fig. 4b), then we use this mesh for I.A. modeling to obtain the mesh of the initial billet (Fig. 4c). We note the mesh of the initial billet obtained by I.A. is very similar to that of Abaqus.

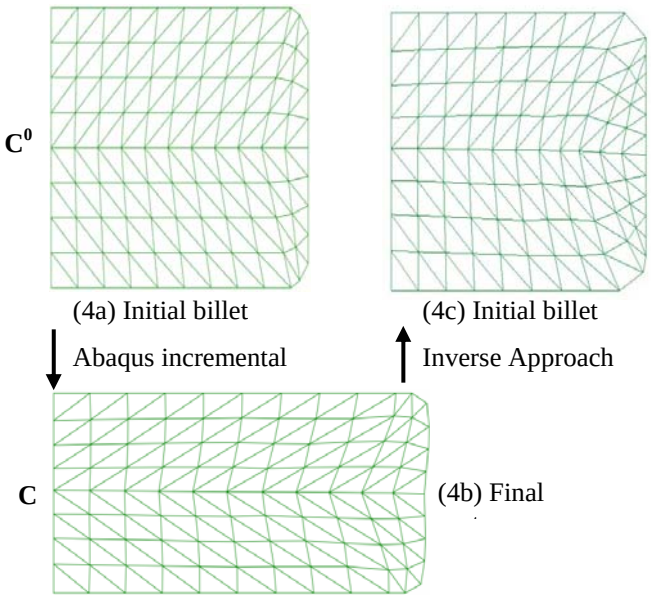

Fig. 4 Initial and final meshes of the part 1

The distributions of the equivalent plastic strain obtained by the Inverse Approach and Abaqus are shown in Fig. 5. We note that the distributions are similar and the maximal and minimal values are in good agreement.

B. *Numerical results of the part 2*

The second axi-symmetric (Fig. 6) has a horizontal plane of symmetry. The half section is meshed with 889 axi-symmetric triangle elements (CAX3 of Abaqus, Fig. 7).

The material properties of the billet are: Young's modulus E=10300 (MPa), Poisson's ratio ν=0.3, friction coefficient μ=0.15, Hollomon stress-strain curve $\bar{\sigma}=140\left(\bar{\varepsilon}^{p}\right)^{0.2}$ (MPa). The punch travel is 3.72 (mm).

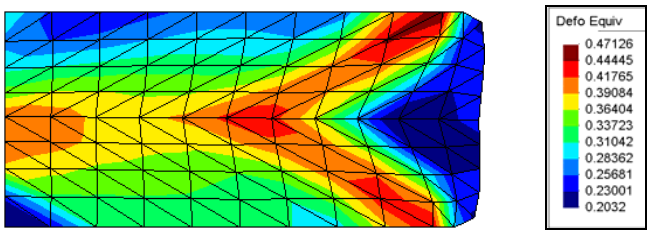

a. Inverse Approach

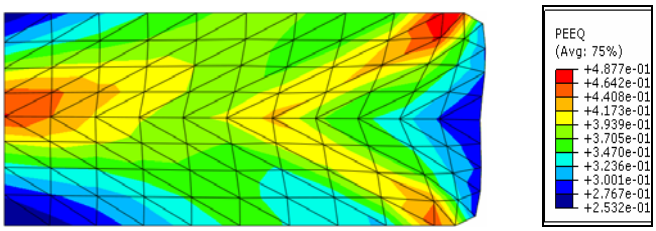

b. Abaqus (Incremental Approach)

Fig. 5 Equivalent plastic strain obtained by I.A. and Abaqus

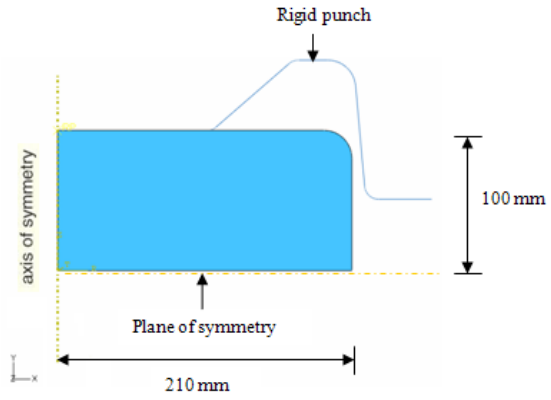

Fig. 6 Geometry of the part 2

ISBN: 978-988-18210-7-2
ISSN: 2078-0958 (Print); ISSN: 2078-0966 (Online)

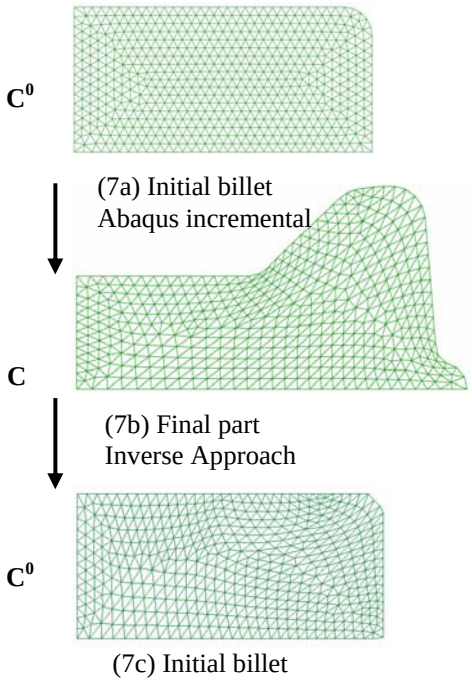

Fig. 7 Initial and final meshes of the part 2

The mesh of the initial billet and the mesh of the final part obtained by Abaqus are shown by Fig. 7a and 7b. Then we use the mesh 7b for the I.A. modeling which gives the mesh of the initial billet (Fig. 7c). A fairly good agreement is observed between the two meshes (Fig. 7a and 7c).

Fig. 8 shows the distributions of the equivalent strain obtained by the Inverse Approach and Abaqus incremental approach. Comparing the equivalent strain distributions obtained by the both approaches, one observes that the equivalent plastic strain distributions are quantitatively very close to each other. The maximum plastic equivalent strains are respectively 0.97 and 1.02. The percentage error is reasonably acceptable (5.2 %).

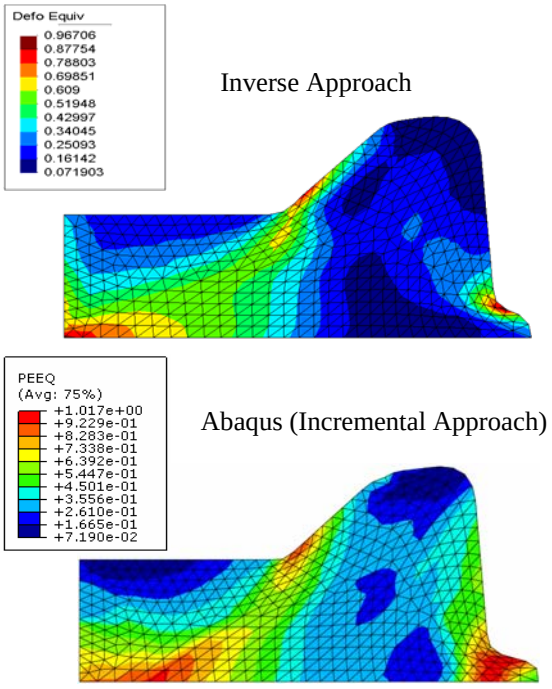

Fig. 8 Equivalent plastic strain obtained by I.A. and Abaqus

V. CONCLUSION

A simplified method called "Inverse Approach" (I.A.) is developed for the axi-symmetrical cold forging modeling. The approach is based on the knowledge of the shape of the final part. The assumptions of the proportional loading and the simplified tool actions make the calculation of the I.A. very fast.

The strain equivalent results obtained by the Inverse Approach are less accurate, but very close to those obtained by the Abaqus incremental approach. The Inverse Approaches is very advantageous to quickly realize the preliminary perform design and optimize the process parameters.

Some limitations of the I.A. are observed. The assumptions on the constitutive law and the tool actions are questionable; they cannot provide good stress estimation because of neglecting the loading history. For complex parts in very large deformation, the remeshing operation and a more powerful resolution algorithm should be considered.

The future work for the I.A. in the forge application is to improve the stress estimation. Recently, a new approach called "Pseudo Inverse Approach" has already been proposed by Guo et al. [9] for the sheet for sheet forming, which keeps the advantages of the I.A. but gives good stress estimation with the loading history consideration, will be tried for the forge application.

ACKNOWLEDGMENT

The collaboration of our partner the University of Technology of Troyes is gratefully acknowledged.

REFERENCES

[1] G. Dhatt, G. Touzot, "*Une présentation de la méthode des éléments finis*", 2e edition, MALOINE S.A. Editor, 1984.
[2] J.L. Batoz, G. Dhatt, "*Modélisation des structures par éléments fini*", Vol. 1, *Solides élastiques*, Editeur HERMES, Paris, 1990.
[3] J.L. Batoz, G. Dhatt, "*Modélisation des structures par éléments fini*", Vol. 3, *Coques*, Editeur HERMES, Paris, 1990.
[4] Bohatier C., Chenot, J.L., "Finite element formulation for non steady state viscoplastic deformation", *Int. J. Meth. Eng.,* 21, pp.1697-1708, 1985.
[5] Kobayashi S., Oh S.I., Altan T., "*Metal forming and finite element method*", Oxford University Press, 1989.
[6] Zhao G., Wright E., Grandhi R.V., "Forging perform design with shape complexity control in simulating backward deformation", *Int. J. Mach. Manuf.,* Vol 35-9, pp. 1225-1239, 1995.
[7] Fourment L., Chung S.H., "Direct and adjoint differentiation methods for shape optimization in non-steady forming application", *European Conference on Computational Mechanics*, Cracow, 2001.
[8] Guo Y.Q., Batoz J.L., Detraux, J.M., Duroux, P., "Finite element procedures for strain estimations of sheet metal forming parts", *Int. J. for Num. Methods in Eng*., Vol. 30, pp. 1385-1401, 1990.
[9] Gati, W., Guo Y.Q., Naceur H., Batoz J.L., "Approche pseudo inverse pour estimation des contraintes dans les pièces embouties axisymétriques", *Revue Européenne des Eléments Finis*, Vol. 12, n° 7-8, pp. 863-886, 2003.

ISBN: 978-988-18210-7-2
ISSN: 2078-0958 (Print); ISSN: 2078-0966 (Online)